ESC Europace (2026) **28**, euag015
https://doi.org/10.1093/europace/euag015

CLINICAL RESEARCH

# Deep learning to predict left ventricular hypertrophy from the electrocardiogram

**Hafiz Naderi [1,2†], Thomas Kaplan[1†], Stefan van Duijvenboden [1,3], Esmeralda Ruiz Pujadas [4], Nay Aung [1,2], C. Anwar A. Chahal [1,2,5,6], Karim Lekadir [4,7], Bishwas Chamling [8,9,10], Marcus Dörr [9,11], Marcello R. P. Markus [8,9,10], Steffen E. Petersen [1,2‡], Julia Ramírez [1,12,13‡], and Patricia B. Munroe [1*‡]**

[1]William Harvey Research Institute, Queen Mary University of London, Charterhouse Square, London, EC1M 6BQ, UK; [2]Barts Heart Centre, St Bartholomew's Hospital, Barts Health NHS Trust, West Smithfield, London, UK; [3]Big Data Institute, La Ka Shing Centre for Health Information and Discovery, University of Oxford, Oxford, UK; [4]Faculty of Mathematics and Computer Science, University of Barcelona, Barcelona, Spain; [5]Centre for Inherited Cardiovascular Diseases, WellSpan Health, Lancaster, PA, USA; [6]Department of Cardiovascular Diseases, Mayo Clinic, Rochester, MN, USA; [7]Institució Catalana de Recerca i Estudis Avançats (ICREA), Barcelona, Spain; [8]Department of Internal Medicine B, University Medicine Greifswald, Greifswald, Germany; [9]German Center for Cardiovascular Research (DZHK), Partner Site Greifswald, Greifswald, Germany; [10]German Center for Diabetes Research (DZD), Partner Site Greifswald, Greifswald, Germany; [11]Institute for Community Medicine, SHIP/KEF, University Medicine Greifswald, Greifswald, Germany; [12]Aragón Institute of Engineering Research, University of Zaragoza, Zaragoza, Spain; and [13]Centro de Investigación Biomédica en Red—Biomateriales, Bioingeniería y Nanomedicina, Zaragoza, Spain

*Received 17 October 2025; accepted after revision 20 January 2026; online publish-ahead-of-print 23 January 2026*

**Aims** Left ventricular hypertrophy (LVH) is a strong predictor of cardiovascular disease. We previously compared supervised machine learning techniques to classify cardiac magnetic resonance (CMR)-derived LVH using electrocardiogram (ECG) and clinical variables in 37 534 UK Biobank participants, obtaining an area under the receiving operating curve (AUROC) of 0.85, but with limited specificity and requiring external validation. In this study, we develop a deep learning (DL) model to improve classification with external evaluation in the Study of Health in Pomerania (SHIP).

**Methods and results** We analysed 12-lead ECGs of 48 835 participants from the UK Biobank imaging study. The dataset was split into a training set (70%), validation set (15%), and test set (15%) for performance evaluation. The model architecture was a fully convolutional network, for which the input was the participants' median ECG and clinical variables and the predicted indexed left ventricular mass (iLVM) as the output. A subsequent logistic regression model was used to recalibrate iLVM predictions. In UK Biobank, 717 (1.5%) participants had CMR-derived LVH and the AUROC for the DL model was 0.97. The ECG components most predictive of LVH were the QRS complex and ventricular rate. The DL model outperformed our supervised algorithms, previous DL modelling efforts and clinical ECG benchmarks. There was modest generalizability of the DL model to 1423 participants in SHIP (AUROC 0.78), with differences in clinical profile, ECG acquisition, and CMR labelling as important factors.

**Conclusion** Our findings support the feasibility of scalable DL-based screening tools for the prediction of LVH from the ECG, whilst highlighting the need for model development using larger datasets with greater diversity to ensure generalizability.

* Corresponding author. *E-mail address*: p.b.munroe@qmul.ac.uk.
† Joint first authors.
‡ Joint last authors.

## Graphical Abstract

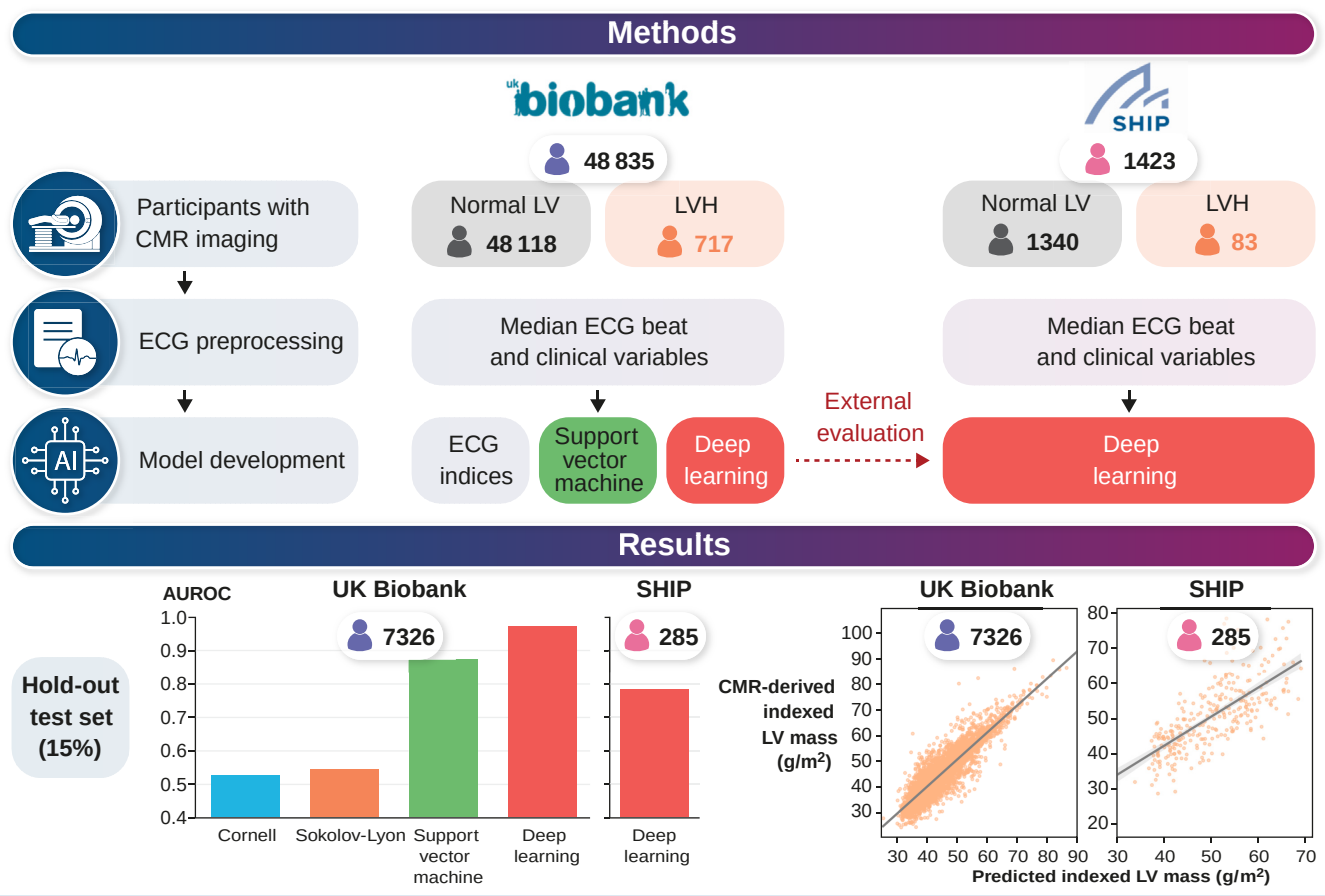


**Keywords** Left ventricular hypertrophy • Electrocardiogram • Deep learning • Machine learning

## What's new?

- In this study, we developed a fully convolutional deep learning (DL) model integrating 12-lead electrocardiogram (ECG) and clinical data to predict cardiac magnetic resonance-derived left ventricular hypertrophy (LVH) in UK Biobank (AUROC 0.97), outperforming our supervised models, previous DL-based efforts and conventional ECG criteria.
- Demonstrated modest but promising generalizability in external evaluation (AUROC 0.78), highlighting domain shift challenges.
- Our findings support the feasibility of developing scalable DL-based screening tools for the prediction of LVH from the ECG.

# Introduction

Left ventricular hypertrophy (LVH) is an established independent risk factor for adverse cardiovascular events.[1,2] Early detection of LVH enables timely intervention and risk stratification, yet it remains underdiagnosed due to limitations in current diagnostic approaches.[3] In clinical practice, the 12-lead electrocardiogram (ECG) is the most accessible and widely used diagnostic tool for detecting LVH. Despite its ubiquity, the ECG has limited sensitivity in identifying LVH when using conventional criteria such as the Sokolow–Lyon or Cornell voltage indices.[4,5] Imaging modalities such as echocardiography and cardiac magnetic resonance (CMR) imaging offer more accurate structural characterization; however, they are resource-intensive and less feasible for large-scale screening.

In previous work, we compared supervised machine learning techniques to classify CMR-derived indexed left ventricular mass (iLVM).[6] We showed that a set of 23 ECG biomarkers with physiological association with LVH, and clinical variables could classify LVH in 37 534 UK Biobank (UKB) participants with an area under the receiver operator curve (AUROC) of 0.85. These are promising results; however, there remains room to enhance diagnostic accuracy for detecting LVH. Recent advances in machine learning have shown promise in augmenting ECG interpretation by uncovering features beyond human perception. Deep learning (DL) models have successfully been applied to identify a range of cardiovascular conditions directly from raw ECG waveforms, including impaired ejection fraction,[7] atrial fibrillation,[8] and hypertrophic cardiomyopathy.[9] These methods leverage the rich information embedded in the ECG signal to detect subtle physiological signatures associated with structural heart disease, with the added potential to reveal unidentified ECG features. Studies using DL applied to the ECG

for LVH prediction in UKB have been reported with modest diagnostic performance in earlier releases of the UKB imaging cohort, achieving a c-statistic of 0.65[10] ($N$ = 32 239) and an AUROC of 0.72[11] ($N$ = 38 686).

In this study, we explore agnostic approaches to improve LVH classification and develop a DL model to predict CMR-derived LVH from the 12-lead ECG and clinical variables using the updated UKB cohort ($N$ = 48 835). We assess the model's diagnostic performance by comparing our approach to previous studies using DL, our supervised machine learning methods and conventional ECG clinical benchmarks. We also evaluate the model's performance in an external population cohort with CMR-derived iLVM annotations.

# Methods

This study adheres to the European Heart Rhythm Association (EHRA) AI checklist, which is provided in Supplementary data.[12]

## Sample selection

The primary sample used for model development and evaluation consisted of 48 835 participants from the baseline UKB imaging study with paired CMR and ECG data. Left ventricular hypertrophy was characterized using CMR parameters derived using an existing analysis pipeline,[13,14] whereby DL models were trained to automatically annotate the LV myocardium and hence derive CMR parameters. The UKB dataset was split into a training set (70%), validation set (15%), and hold-out test set (15%) for performance evaluation. The key CMR parameter of interest was LVM. Indexing with respect to body surface area was performed with the Mostellar formula.[15] Left ventricular hypertrophy was defined as iLVM > 70 g/m$^2$ (males) and > 55 g/m$^2$ (females) with respect to normal ranges published for the UKB imaging study,[13] corresponding to the thresholds in which sex-specific iLVM exceeds the 95% prediction interval for at least one of their reference age groups. To assist in interpretations of our results, we derived potential causes of LVH in these participants (*Table 1*): Hypertension, based on diagnoses, medication, and measurements (described in 'Clinical variables' section); hypertrophic cardiomyopathy, as the presence of rare coding variants (minor allele frequency < 0.00004) in eight implicated genes using whole exome sequence data and potential phenocopies (Fabry disease, amyloidosis, glycogen storage diseases, and RSAopathies).[16,17]

## ECG processing

A 12-lead ECG was performed for participants of the UKB imaging study on the same day as the CMR imaging. We analysed the median heartbeat waveform across eight independent ECG leads (I, II, and V1–6), derived from the raw 15 s signals. The median beats were calculated by a classical method: initial bandpass Butterworth filtering between 1 and 45 Hz; peak-picking to identify R waves from the ECG principal components; beat alignment using time-lagged cross-correlation, with filtering of uncorrelated beats; and final averaging of retained beat waveforms. Given the use of a signal-averaged ECG waveform, the mean R-R interval (ventricular rate) was included as the only ECG biomarker in participant metadata (i.e. alongside the clinical variables defined in the following section).

## Clinical variables

Several clinical variables associated with LVH were included as metadata (*Table 1*). Clinical variables were derived using a combination of self-reported questionnaires performed at the imaging assessment visit, formal diagnoses and medications linked from primary care, physical measures, and biochemistry. Disease associations included hypertension, hypercholesterolaemia, and diabetes mellitus. Blood pressure (BP) measurements were averaged across readings taken at the imaging assessment centre visit. If participants were taking BP-lowering medication, their averaged (manual) BP readings were adjusted by adding either 15 mmHg to systolic BP or 10 mmHg to diastolic BP as per previous work.[18] Hypertension was further defined based on formal diagnoses and the use of BP medication, or BP levels exceeding a 130/85 mmHg cut-off. Diabetes mellitus was determined by haemoglobin A1c (HbA1c) ≥ 48 mmol/mol. Hypercholesterolaemia was defined by serum total cholesterol of ≥ 5 mmol/L, having corrected for cholesterol-lowering medication by dividing total and non-HDL cholesterol by 0.73 and 0.66, respectively.[19] As noted in the previous section, the mean R-R interval was included as a sole ECG biomarker alongside other clinical variables.

## Model architecture

We evaluated a performant network architecture for time series classification, a Fully Convolutional Network (FCN).[20] The FCN serves as an effective baseline architecture that has been demonstrated to perform accurate classification across a range of multivariate time series datasets, even compared with state-of-the-art approaches.[21] Our FCN consisted of three convolutional blocks, but convolutional parameters and operations included in each block were selected through hyperparameter optimization (described in 'Training framework' section). As part of this optimization, we evaluated the inclusion of max pooling layers to reduce overfitting, and batch normalization to speed up convergence whilst improving model generalization. A global average pooling (GAP) layer was used after the convolutions, drastically reducing the number of weights (parameters) used to represent the ECG features. The GAP output is concatenated with participant metadata before passing through two fully connected layers, which were also parameterized through optimization.

In addition to the FCN, we evaluated an open-source Residual Network (ResNet) as the most performant architecture of many for a related task—classifying hypertrophic cardiomyopathy for participants with hypertension.[22] We evaluated their optimal configuration, a large 34-layer ResNet (ResNet34), to assess the potential performance implication of using a larger DL architecture (~7.5 M parameters as opposed to ~ 293k), including common optimizations for ECG modelling (residual connections).[23] The ResNet34 was modified similarly to the FCN to include an output head for which the participant metadata was concatenated with ECG features output by the convolutional blocks. The model was implemented using Python v3.11.11 and PyTorch v2.6.0 (CPU-only). The versions of other Python dependencies are made available via the linked code repository.[24,25]

## Model configurations

We trained separate models to predict CMR-derived LVH (binary classification) and iLVM (g/m$^2$); and henceforth, when referring to LVM, we will be referring to the indexed version of the measurement. Models were named based on their target variable, $\text{FCN}_{\text{LVH}}$ and $\text{ResNet34}_{\text{LVH}}$ for binary classification of CMR-derived LVH from the ECG, or $\text{FCN}_{\text{LVM}}$ and $\text{ResNet34}_{\text{LVM}}$ for regression over CMR-derived LVM from the ECG. Additionally, variants of each model were trained with and without inclusion of participant metadata (i.e. clinical variables), such that the output heads of each model consisted solely of fully connected layers with ECG features as input—it was previously found that clinical metadata did not improve DL discrimination of LVH within UKB.[10]

## Preprocessing

Median ECG waveforms were transformed to millivolts (mV) to shift the distribution closer to that of a unit interval. Continuous-valued features were scaled and translated into a unit interval relative to the training partition of the UKB cohort (min-max normalization). The smoking status variable was re-encoded in multiple columns for each of the possible status values (one-hot encoding), whereas other categorical variables were binary and unchanged.

**Table 1** Baseline characteristics of the UKB and SHIP participants

| | UKB (*N* = 48 835) | | | | SHIP (*N* = 1423) | | | | *P* | | |
|---|---|---|---|---|---|---|---|---|---|---|---|
| | All (*N* = 48 835) | LVH (*N* = 717) | Normal LV (*N* = 48 118) | *P* | All (*N* = 1423) | LVH (*N* = 83) | Normal LV (*N* = 1340) | *P* | All | LVH | Normal |
| Age (years) | 65 (7.8) | 64 (7.7) | 65 (7.8) | **0.04** | 52 (13.2) | 52 (11.9) | 52 (13.3) | 0.8 | **<0.001** | **<0.001** | **<0.001** |
| Sex, female (%) | 25 315 (51.8) | 353 (49.2) | 24 962 (51.9) | **0.02** | 653 (45.9) | 32 (38.6) | 621 (46.3) | 0.2 | **<0.001** | 0.1 | **<0.001** |
| BMI (kg/m$^2$) | 26.0 (4.3) | 26.84 (4.9) | 25.99 (4.3) | **<0.001** | 26.94 (4.2) | 27.75 (4.3) | 26.89 (4.2) | 0.2 | **<0.001** | 0.6 | **<0.001** |
| Ethnicity, White European (%) | 47 220 (96.7) | 690 (96.2) | 46 530 (94.4) | 0.5 | 1 423 (100.0) | 83 (100.0) | 1 340 (100.0) | | **<0.001** | 0.1 | **<0.001** |
| Systolic BP (mmHg) | 142.5 (21.2) | 159.0 (23.0) | 142.0 (21.1) | **<0.001** | 127.5 (17.6) | 134.0 (18.7) | 127.0 (17.3) | **<0.001** | **<0.001** | **<0.001** | **<0.001** |
| Diastolic BP (mmHg) | 81.0 (11.4) | 86.00 (13.1) | 81.00 (11.3) | **<0.001** | 78.0 (10.2) | 82.0 (11.5) | 77.8 (10.1) | **0.01** | **<0.001** | **0.001** | **<0.001** |
| Potential causes of LVH (%) | | | | | | | | | | | |
| *Hypertension* | 35 903 (73.5) | 620 (86.5) | 35 283 (73.3) | **<0.001** | 917 (64.4) | 67 (80.7) | 850 (63.4) | **0.001** | **<0.001** | 0.1 | **<0.001** |
| *HCM variant carrier* | 5281 (10.8) | 88 (12.3) | 5193 (10.8) | **<0.001** | | | | | | | |
| *Phenocopies* | 30 (0.1) | 0 (0.0) | 30 (0.1) | | | | | | | | |
| High cholesterol (%) | 31 388 (64.3) | 456 (63.6) | 30 923 (64.3) | 0.7 | 1 039 (73.0) | 60 (72.3) | 979 (73.1) | 0.9 | **<0.001** | 0.2 | **<0.001** |
| *Total cholesterol* (mmol/L) | 4.9 (1.2) | 4.9 (1.1) | 4.96 (1.2) | **0.02** | 5.4 (1.1) | 5.50 (1.2) | 5.40 (1.1) | 0.5 | **<0.001** | **<0.001** | **<0.001** |
| *Non-HDL cholesterol* (mmol/L) | 3.5 (1.2) | 3.5 (1.1) | 3.5 (1.2) | 0.1 | 3.9 (1.1) | 4.06 (1.2) | 3.97 (1.1) | 0.9 | **<0.001** | **0.003** | **<0.001** |
| Diabetes (%) | 2 738 (5.6) | 57 (7.9) | 2 681 (5.6) | **0.01** | 104 (7.3) | 9 (10.8) | 95 (7.1) | 0.1 | **0.01** | 0.4 | **0.02** |
| Smoking status (%) | | | | | | | | | | | |
| *Never* | 29 780 (61.0) | 419 (58.4) | 29 361 (61.0) | 0.2 | 0 (0) | 0 (0) | 0 (0) | | **<0.001** | **<0.001** | **<0.001** |
| *Previous* | 16 360 (33.5) | 238 (33.2) | 16 122 (33.5) | 0.9 | 1 118 (78.6) | 60 (72.3) | 1058 (78.9) | 0.2 | **<0.001** | **<0.001** | **<0.001** |
| *Current* | 2 695 (5.5) | 60 (8.4) | 2 635 (5.5) | **0.002** | 304 (21.4) | 23 (27.7) | 281 (20.9) | 0.2 | **<0.001** | **<0.001** | **<0.001** |
| Alcohol intake status (%) | | | | 0.9 | | | | | 0.6 | 0.8 | 0.54 |
| *Never* | 2 578 (5.3) | 36 (5.0) | 2 542 (5.3) | | 79 (5.5) | 3 (3.6) | 76 (5.7) | 0.6 | | | |
| *Current* | 46 257 (94.7) | 681 (94.9) | 45 576 (94.7) | | 1 344 (94.5) | 80 (96.4) | 1 264 (94.3) | 0.6 | | | |
| Ventricular rate (beats/min) | 61.7 (10.2) | 59.3 (10.8) | 61.7 (10.2) | **<0.001** | 63.3 (10.4) | 61.48 (9.9) | 63.29 (10.5) | **0.03** | **<0.001** | 0.1 | **<0.001** |
| LVM (*g*) | 82.5 (22.2) | 131.4 (32.3) | 82.0 (21.2) | **<0.001** | 96.3 (26.2) | 145.25 (28.6) | 93.82 (24.1) | **<0.001** | **<0.001** | 0.2 | **<0.001** |
| Indexed LVM (g/m$^2$) | 44.0 (8.4) | 70.4 (10.5) | 43.8 (7.9) | **<0.001** | 49.3 (9.9) | 71.72 (9.2) | 48.34 (8.8) | **<0.001** | **<0.001** | 0.5 | **<0.001** |

BMI: body mass index, BP: blood pressure, HCM: hypertrophic cardiomyopathy, HDL: high-density lipoprotein, LVH: left ventricular hypertrophy, LVM: left ventricular mass, SHIP: Study of Health in Pomerania, UKB: UK Biobank.

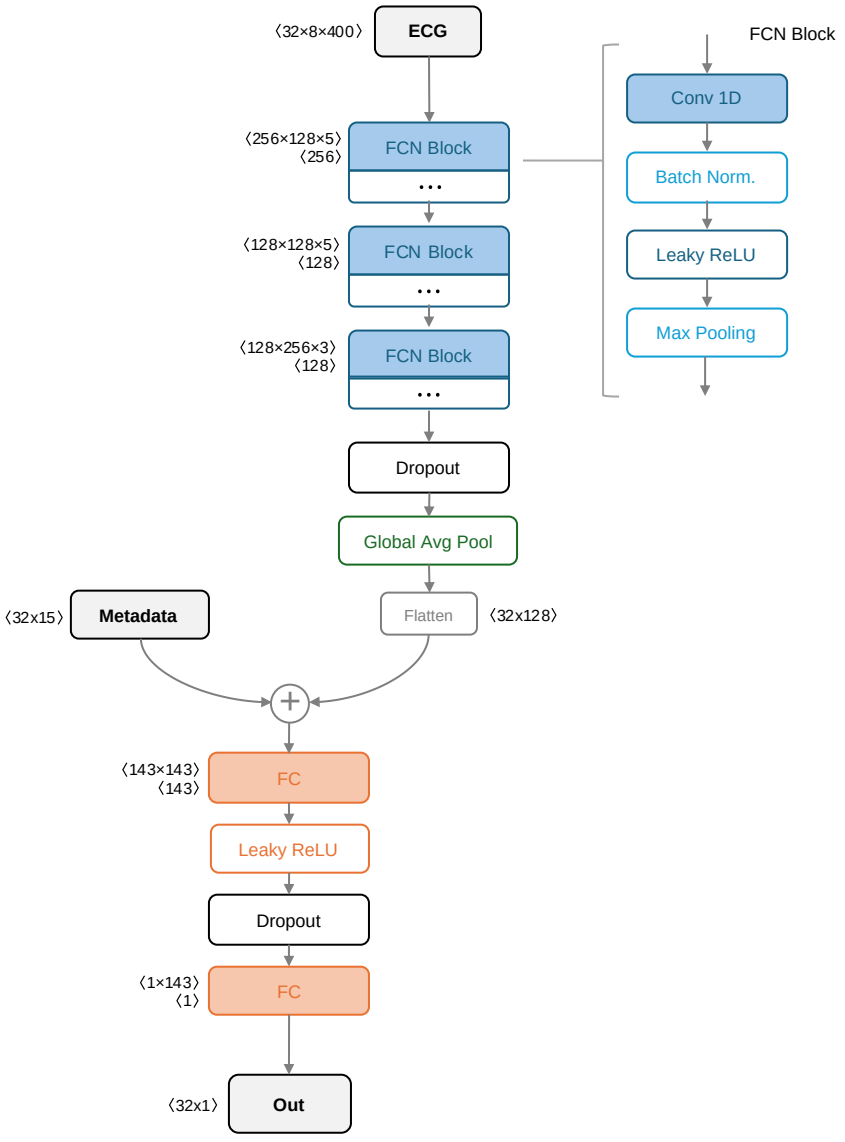


**Figure 1** Fully convolutional network (Wang et al., 2016) architecture used in the present work, consisting of three convolutional blocks, the output of which is pooled and concatenated with clinical metadata and output through two fully connected layers for final predictions.

## Training framework

The UKB cohort's validation split was used to determine when the model performance had stopped improving, with an early stopping criterion of 20 epochs without improvement, and learning rate reduction by a factor of 0.1 when the model had not improved within 10 epochs. For all model configurations analysed, training terminated within 200 epochs. To reduce sensitivity to errors from outliers, we used the logarithm of hyperbolic cosine (log-cosh) as a loss function in predicting LVM, i.e. improving robustness of training given the long-tailed LVM distribution. Hyperparameter optimization was performed for the FCN architecture using a variant of the Hyperband algorithm (Tune).[26] Optimizations for the learning process were the optimizer used (Adam or stochastic gradient descent), learning rate {1e-4, 5e-4, 1e-3, 1e-2} and batch size {16, 32, 64, 128}. The selected training parameters resulting in optimal validation losses were the Adam optimizer with a learning rate of 5e-4 and batch size of 64.

Optimizations for the FCN included the general convolution configuration (filter count and length), which either followed the configuration proposed by Wang et al. (2016) or a smaller but compatible configuration used by Zhou et al. (2024) for encoding similar median ECG waveforms from UKB.[20,27] We additionally optimized for: use of batch-normalization within convolutional blocks; use of max pooling within convolutional blocks; dropout after the convolutional layer (probability $P = 0, 0.1, ..., 0.8$); dropout after the first fully connected layer (probability $P = 0, 0.1, ..., 0.8$); and the inclusion of metadata. The selected configuration resulting in optimal validation losses was that of Wang et al. (2016), with the addition of batch normalization and max-pooling layers within each convolutional block; a dropout of 0.4 after the convolutional layers; a dropout of 0.6 between the fully connected layers; and the inclusion of metadata.[20] The FCN network architecture is illustrated in *Figure 1*.

## Left ventricular hypertrophy classification

Further to the $FCN_{LVH}$, which directly classified participants with LVH or normal LV mass, iLVM predictions output by the $FCN_{LVM}$ were used to derive LVH cases in two ways. First, using the iLVM

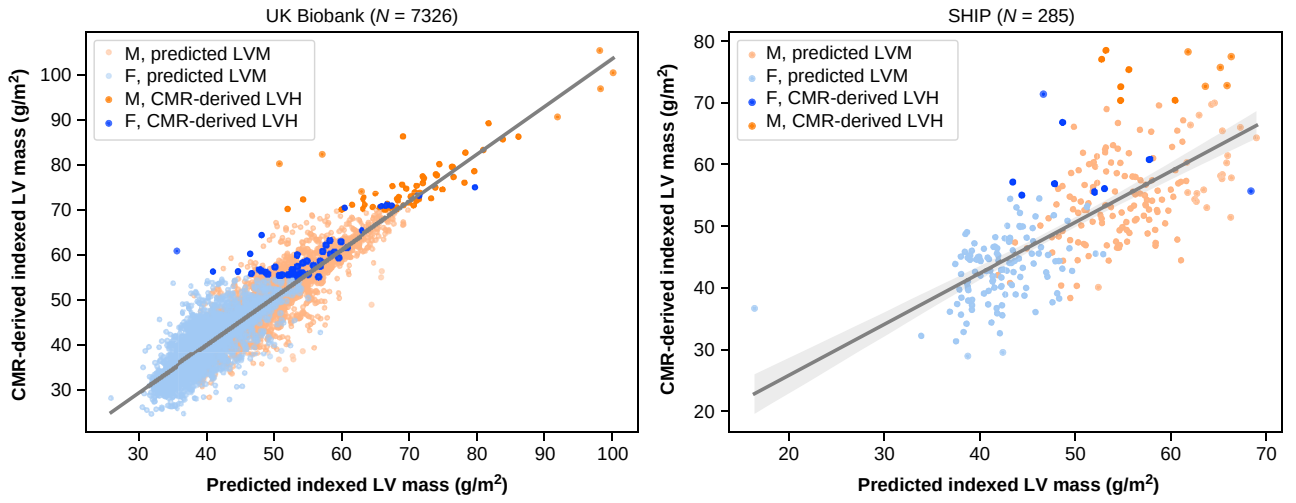


**Figure 2** Correlation between predicted indexed LVM and CMR-derived indexed LVM in UKB and SHIP test sets. Diagonal lines are linear OLS fits with shaded confidence intervals (95%). CMR, cardiac magnetic resonance; LVM, left ventricular mass; OLS, ordinary least squares; SHIP, Study of Health in Pomerania; UKB, UK Biobank.

cut-offs previously specified. Secondly, iLVM predictions were inputted into a separate logistic regression (LR) model, which learned to classify instances of LVH, allowing for custom decision thresholds (in terms of iLVM) that diverge from published ranges, i.e. a linear recalibration that compensates for systematically skewed predictions reflecting the imbalanced ground-truth iLVM distribution. Sex was also input to the LR as a single covariate, given the significant iLVM difference between sexes according to reference ranges derived from CMR in UKB.[13] Together, the FCN and LR ($FCN_{LVM}$ + LR) pipeline provides an opaque LVH classification that can be compared with the other two methods. Sample weights for the LR model were balanced according to class frequencies to account for the class imbalance between LVH and normal LV cases.

## Performance benchmarks

As baseline performance benchmarks, we used our previous supervised methods from the existing literature for the classification of LVH, which outperformed the only existing DL approach for LVH classification within the UKB cohort.[6,10] In addition to the aforementioned clinical variables, these supervised methods were trained using an extensive set of ECG biomarkers (e.g. QRS duration, QRS wave amplitude, and pathological Q waves) extracted automatically using signal processing. The most performant model was an optimized support vector machine (SVM), using a radial basis function kernel with a regularization constant $C = 1$. This was re-implemented and trained on identical splits of our present dataset, using random under-sampling consistently to balance against the minority class (LVH). The original ECG feature extraction pipeline used was run on the ECGs that were not part of their original cohort. The same cohort splits were used to train the SVM. Notably, the validation set was used to perform a five-fold cross-validation grid search over hyperparameters, to ensure it was not possible to identify an updated parameter set outperforming that selected in the original work. We also evaluated two clinically used ECG criteria for LVH, calculated with the ECG biomarkers extracted using the pipeline noted above: Sokolow–Lyon and Cornell voltage.[28,29]

## External evaluation

The Study of Health in Pomerania (SHIP) was used for the external evaluation of the models trained in UKB. Study of Health in Pomerania is a study investigating common risk factors in a random sample of the population from West Pomerania, Northeastern Germany.[30] A total of 1474 participants drawn from the baseline SHIP-TREND-0 cohort and second follow-up SHIP-START-2 cohorts were studied in the present work, given the availability of paired CMR and 12-lead ECG data. Electrocardiograms were processed from EDF files, using PyEDFlib, before processing consistent with that of the UKB ECGs.[31] There were only six missing fields across a total of four participants in SHIP, which were imputed using either mode or median imputation for binary or continuous columns, respectively: two systolic BP, two diastolic BP, one total cholesterol level, and one smoking status.

Given the limited UKB sample available for model training and the differing cohort characteristics compared with SHIP (*Table 1*), the DL models pre-trained on UKB data were fine-tuned in SHIP to mitigate domain shift effects and improve generalizability.[32] The SHIP dataset was split into a training set (60%), validation set (20%), and hold-out test set (20%) for performance evaluation. Given the small size of the cohort, we performed random data augmentation for the training set: random crops at the start and end of all leads (uniform sampling of up to 25 samples for each end), followed by linear interpolation; random Gaussian noise per lead ($M = 0$, $SD = 0.005$); and minor amplitude scaling across leads (uniform sampling between [0.9, 1.1]). The augmentations used were selected to preserve ECG morphology. The same optimizer (Adam) was used for fine-tuning, with additional parameter weight-decay (regularization) to reduce overfitting. Layers were incrementally unfrozen for fine-tuning, starting with the output heads (learning rate 5e-5, weight-decay 1e-4), and then each convolutional block (learning rate 1e-4, weight-decay 1e-5).

## Statistical analyses

For classification performance analyses, confidence intervals for AUROC were calculated analytically.[33,34] Significant differences in AUROC were calculated using a fast implementation of DeLong's algorithm.[35] Sensitivity and specificity were reported at operating points where the difference between TPR and FPR (Youden's J statistic) is maximal, i.e. an optimized decision threshold. Regression performance was assessed using the Pearson correlation coefficient, linear regression using the ordinary least squares (OLS) method and Bland–Altman agreement. Accuracy was reported in terms of mean absolute error (MAE) and mean error (ME) with 95% confidence intervals computed via bootstrapping ($N = 5000$).

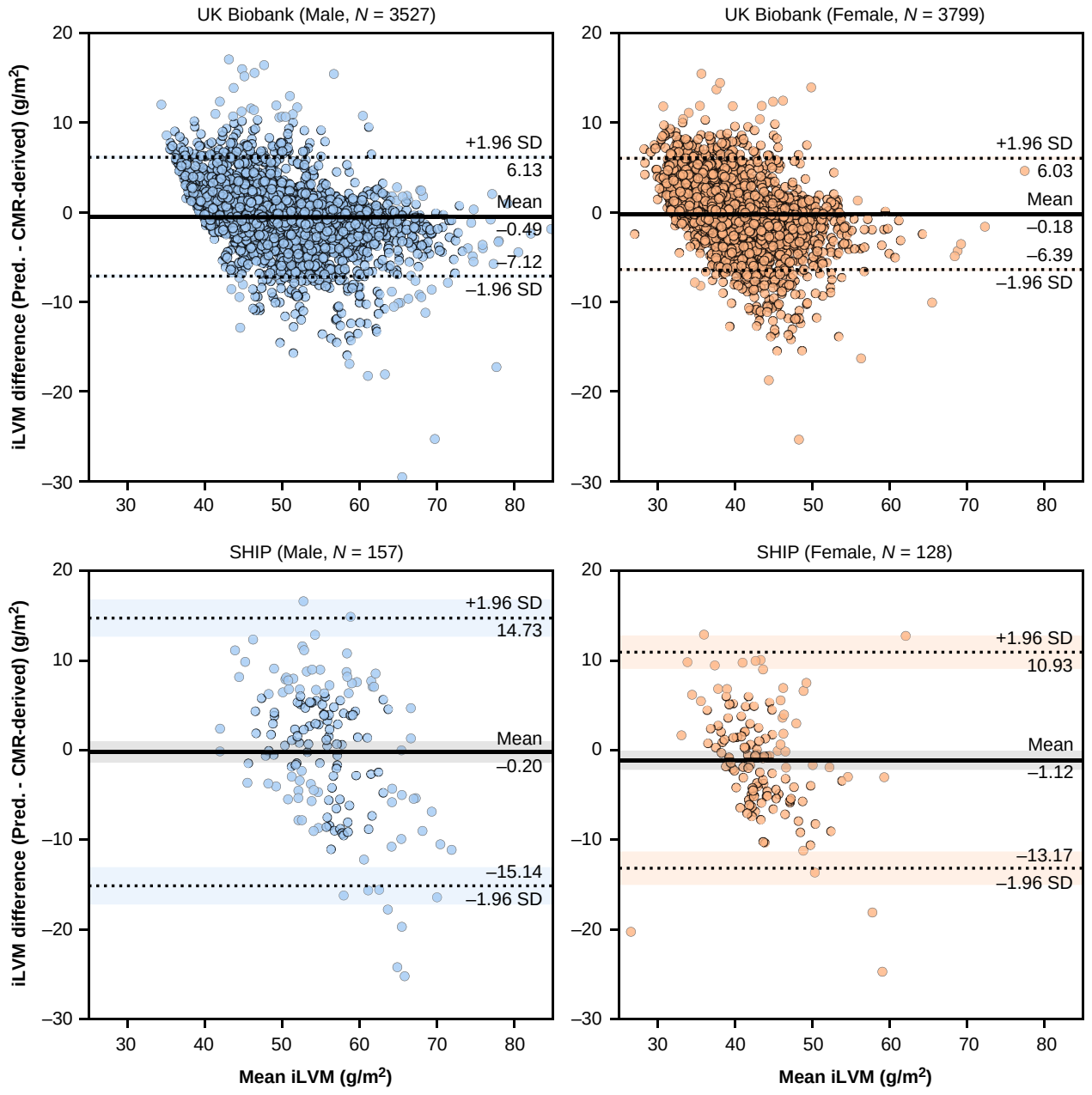


**Figure 3** Bland–Altman plots demonstrating pairwise agreement of predicted indexed LVM and CMR-derived LVM in UKB and SHIP test sets, by sex. Horizontal dashed lines indicate upper and low limits of agreement (95%) and the respective shaded confidence intervals (95%). CMR, cardiac magnetic resonance; LVM, left ventricular mass; SHIP, Study of Health in Pomerania; UKB, UK Biobank.

## Model explainability

The importance of ECG regions and clinical variables to model predictions was assessed using the Integrated Gradients feature attribution method, as implemented in the SHapley Additive exPlanations package (SHAP, v0.47.1).[36,37] Integrated Gradients resemble SHAP values but use the gradients operator of a deep neural network to identify salient input features with respect to some background (baseline) sample—for which we use a large random sampling of $N = 1000$ participants' ECGs and clinical metadata to avoid possible instability of the analyses.[38] Put simply, integrated gradients SHAP evaluates how sensitive the DL model predictions are to changes in the input features. We report feature importances at a local level, for participants with predicted iLVM below or above the 5th and 95th percentiles, respectively, i.e. extremes of both measures, to illustrate the most informative clinical variables and ECG features. Whilst the method was applied at a local level, it also offers individual-level explainability (e.g. saliency of an individual ECG waveform).

# Results

## Study populations

The characteristics of the UKB participants ($N = 48\,835$) and the external evaluation cohort ($N = 1423$), the Study of Health in Pomerania (SHIP), are shown in *Table 1*. Compared to UKB, the

**Table 2** LVH classification performance in UKB the FCN variants (present work), SVM (replication of Naderi et al., 2023), criteria for Sokolow–Lyon and Cornell voltage; with 95% confidence intervals in brackets

| Model | AUROC | Sensitivity | Specificity | F1 |
|---|---|---|---|---|
| $FCN_{LVH}$ | 0.88 (0.85, 0.92) | 0.81 (0.73, 0.88) | 0.84 (0.83, 0.84) | 0.52 (0.50, 0.54) |
| $FCN_{LVM}$ | 0.73 (0.68, 0.78) | 0.46 (0.37, 0.56) | 0.99 (0.99, 1.0) | 0.81 (0.79, 0.83) |
| $FCN_{LVM}$ + LR | 0.97 (0.95, 0.99) | 0.92 (0.85, 0.95) | 0.95 (0.95, 0.96) | 0.66 (0.64, 0.68) |
| SVM | 0.87 (0.84, 0.90) | 0.87 (0.79, 0.92) | 0.75 (0.74, 0.76) | 0.47 (0.45, 0.49) |
| Sokolow–Lyon | 0.54 (0.52, 0.57) | 0.10 (0.06, 0.18) | 0.98 (0.98, 0.99) | 0.54 (0.52, 0.56) |
| Cornell voltage | 0.52 (0.49, 0.56) | 0.12 (0.07, 0.20) | 0.92 (0.92, 0.93) | 0.50 (0.48, 0.52) |

AUROC: area under the receiver operator curve, FCN: Fully Convolutional Network, LR: logistic regression, LVH: left ventricular hypertrophy, LVM: left ventricular mass, SVM: support vector machine, UKB: UK Biobank.

**Table 3** LVH classification performance in SHIP for FCN variants; with confidence intervals (95%) in brackets

| Model | AUROC | Sensitivity | Specificity | F1 |
|---|---|---|---|---|
| $FCN_{LVH}$ | 0.78 (0.63, 0.93) | 0.76 (0.53, 0.90) | 0.85 (0.80, 0.89) | 0.64 (0.54, 0.73) |
| $FCN_{LVM}$ | 0.55 (0.48, 0.62) | 0.10 (0.03, 0.30) | 1.0 (0.99, 1.00) | 0.57 (0.48, 0.62) |
| $FCN_{LVM}$ + LR | 0.78 (0.69, 0.88) | 0.65 (0.43, 0.82) | 0.80 (0.74, 0.84) | 0.59 (0.49, 0.68) |

AUROC: area under the receiver operator curve, FCN: Fully Convolutional Network, LR: logistic regression, LVH: left ventricular hypertrophy, LVM: left ventricular mass, SHIP: Study of Health in Pomerania.

SHIP cohort was younger (mean age 65 vs. 52 years, $P < 0.001$), had a slightly lower proportion of females (52% vs. 46%, $P < 0.001$) and a higher prevalence of LVH (1.5% vs. 5.8%, $P < 0.001$) and higher overall iLVM (44 g/m$^2$ vs. 49 g/m$^2$, $P < 0.001$). The most common potential cause of LVH in participants was hypertension (73.5% in UKB and 64.4% in SHIP). A relatively small portion of UKB participants carried rare coding variants for genes implicated in hypertrophic cardiomyopathy (10.8%), with a marginal but significantly higher prevalence in individuals with LVH (12.3% vs. 10.8%, $P < 0.001$). Very few participants were identified with potential phenocopies ($N = 30$, 0.1%).

## Left ventricular mass prediction

Indexed left ventricular mass predictions were accurate (MAE 2.21 g/m$^2$ [2.16, 2.27]) and had a strong correlation with CMR-derived LVM (adj. $R^2 = 0.85$, $P < 0.001$; $r = 0.92$, $P < 0.001$). *Figure 2* reveals that differences in CMR-derived and predicted iLVM were more pronounced in several of the participants with LVH. Generally, iLVM was systematically underestimated (ME −0.33 g/m$^2$ [−0.26, −0.40], skew = −0.41), reflecting the imbalanced CMR-derived iLVM distribution whereby a relatively small sub-population has LVH. Bland–Altman agreement in *Figure 3* better illustrates the heteroscedasticity of iLVM predictions, with a fan-like pattern indicating increasing prediction error at the upper extremes of iLVM (i.e. LVH).

## Left ventricular hypertrophy classification

LVH classification performance is reported in *Table 2*. In terms of AUROC, classification performance was greatest in the $FCN_{LVM}$ + LR (AUROC = 0.97; 95% confidence interval 0.95–0.99), significantly outperforming the SVM model (AUROC = 0.87 [0.84–0.90]). This largely stemmed from improved specificity in the $FCN_{LVM}$ + LR (specificity = 0.95 [0.95–0.96]) compared to the SVM (specificity = 0.75 [0.74–0.76]), despite more comparable sensitivity between the $FCN_{LVM}$ + LR (sensitivity = 0.92 [0.85–0.95]) and SVM (sensitivity = 0.87 [0.79–0.92]). The $FCN_{LVM}$ recorded the highest specificity (specificity = 0.99 [0.99–1.00]), but it did not achieve an AUROC improvement over the SVM, as the LVH diagnoses derived from the pre-determined threshold on predicted iLVM lacked sensitivity due to systematic underestimation. Accordingly, the LR-optimized decision thresholds are shown in Supplementary material online, *Figure S1* (>58.9 g/m$^2$ for males and > 46.9 g/m$^2$ for females), indicating a slight revision of LVH cut-offs compared to our previous publication.[13] The FCN variant directly predicting LVH, $FCN_{LVH}$, achieved a modest diagnostic improvement compared to the SVM. The AUROC curves and optimized operating points are shown in Supplementary material online, *Figure S2*. The AUROC differences between the SVM and FCN variants were statistically significant, DeLong's test $P < 0.001$. Both the SVM and FCNs saw dramatic sensitivity improvements compared to the classical ECG criteria, which were limited for both Sokolow–Lyon (sensitivity = 0.10 [0.06–0.18]) and Cornell voltage (sensitivity = 0.12 [0.07–0.20]) criteria. Support vector machine and FCN variants depend entirely on the ECG (i.e. excluding clinical features) performed comparably to those using both ECG and clinical features (see Supplementary material online, *Table S1*).

## ECG saliency and feature importance

Clinical feature importance in terms of SHAP values is shown in *Figure 4* for participants from the UKB hold-out test partition.

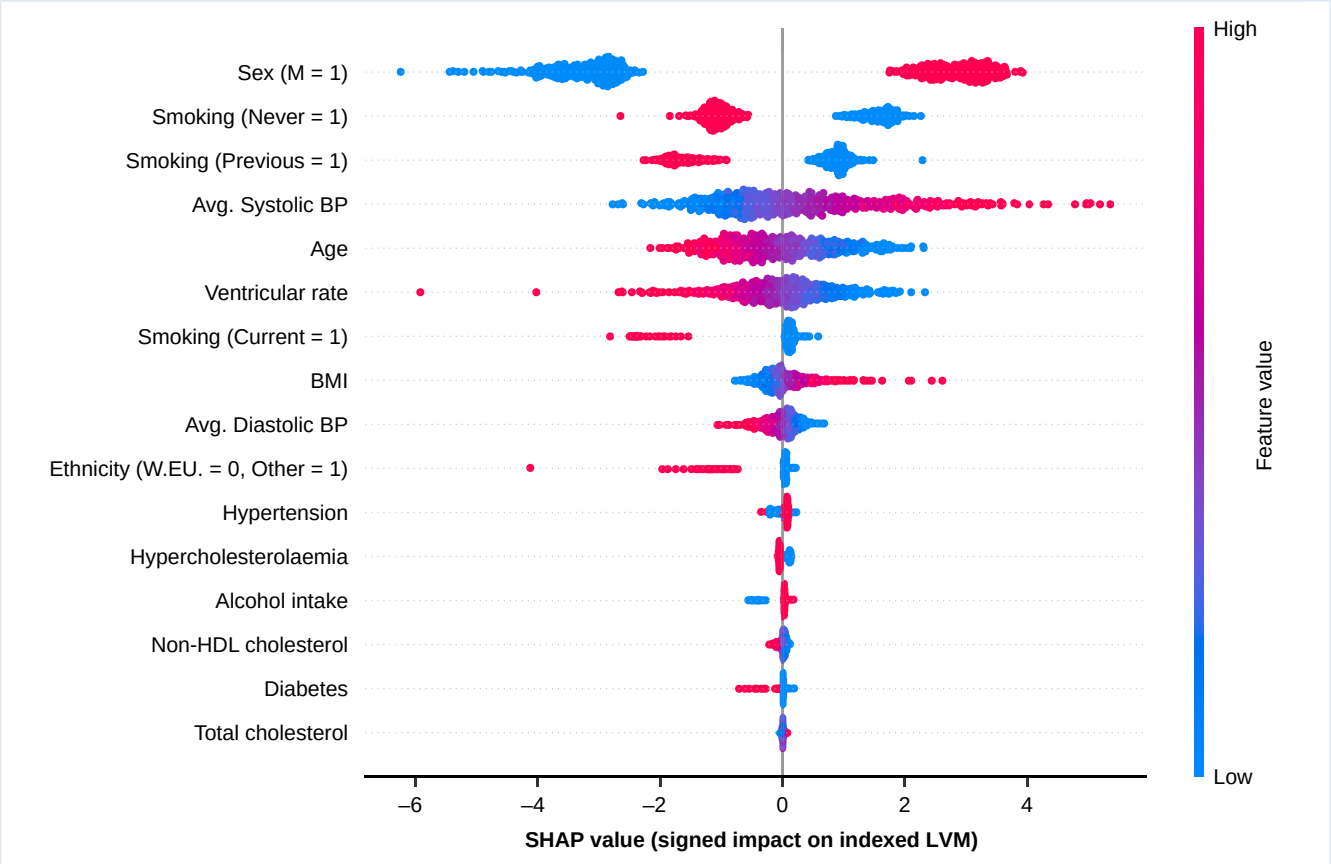


**Figure 4** SHAP feature importance for participants' clinical variables in the UKB test set. Magnitude of SHAP values (x-axis) corresponds to the prediction effect sizes, and direction to increased or decreased prediction values. Colors indicate the variable correlation, higher variable values in red and lower in blue. Binary value encodings are indicated on the label (y-axis), e.g. for sex, male (M) = 1, so shown in red—note the positive SHAP values, larger LVM predictions. LVM, left ventricular mass; SHAP, SHapley Additive exPlanations.

Sex, smoking status, and age were amongst the most predictive features for iLVM, in addition to ventricular rate (our only derived ECG feature), and systolic BP.[10,11] Saliency maps for ECG waveforms (using approximated SHAP values) are shown in *Figure 5* for iLVM, for two examples of participants with low and high predicted iLVM by the $FCN_{LVM}$. Similarly, mean ECGs for individuals with low and high predicted iLVM are shown in *Figure 6*. Generally, the components seemingly most relevant for LVM estimation are the QRS complex and *P*-wave.

## External evaluation in SHIP

The average iLVM prediction error increased (MAE 5.51 g/m$^2$ [5.02, 6.03]), but remained relatively low in absolute terms, with a moderate correlation to CMR-derived iLVM (adj. $R^2$ = 0.50, $P < 0.001$, $r = 0.71$, $P < 0.001$). Similarly to the UKB test set, iLVM was underestimated to a greater extent (ME 0.62 g/m$^2$ [–0.20, 1.43], skew = –0.56). The corresponding correlations are shown in *Figure 2*. Left ventricular hypertrophy detection was moderate (*Table 3*), with a large decrease in AUROC for all FCN configurations, most notably the $FCN_{LVM}$ + LR (AUROC = 0.78 [0.69, 0.88]), which performed more comparably to the $FCN_{LVH}$ (AUROC = 0.78 [0.63, 0.93]), but the relative AUROC distribution for FCN variants in SHIP was broadly similar to that of the UKB test set (*Figure 7*).

# Discussion

In this study, we developed and evaluated a DL model to predict CMR-derived LVH using 12-lead ECG and clinical variables and demonstrated that the DL model outperformed prior machine learning methods and conventional ECG criteria in detecting LVH. External evaluation of the DL model in the SHIP cohort yielded modest generalizability, aligning with findings in other comparable studies, whereby external out-of-sample performance is typically limited.[10,11]

The DL model retained biological plausibility with SHAP analyses showing sex, age, and systolic BP being among the most influential clinical predictors, consistent with known risk factors for LVH. Importantly, the QRS complex and ventricular rate emerged as salient ECG components, supporting the pathophysiological underpinnings of LVH, which affects ventricular depolarization and conduction times.[5,39,40] Clinically, resting heart rate can reflect cardiorespiratory fitness, autonomic tone, and haemodynamic compensation in the context of reduced diastolic filling time or reduced stroke volume with compensatory tachycardia.[41,42] In addition, higher ventricular rates may act as a proxy for comorbidity burden that contributes to LV remodelling, including hypertension, obesity, and subclinical heart failure. Therefore, ventricular rate may represent a surrogate marker capturing correlated physiological stressors and

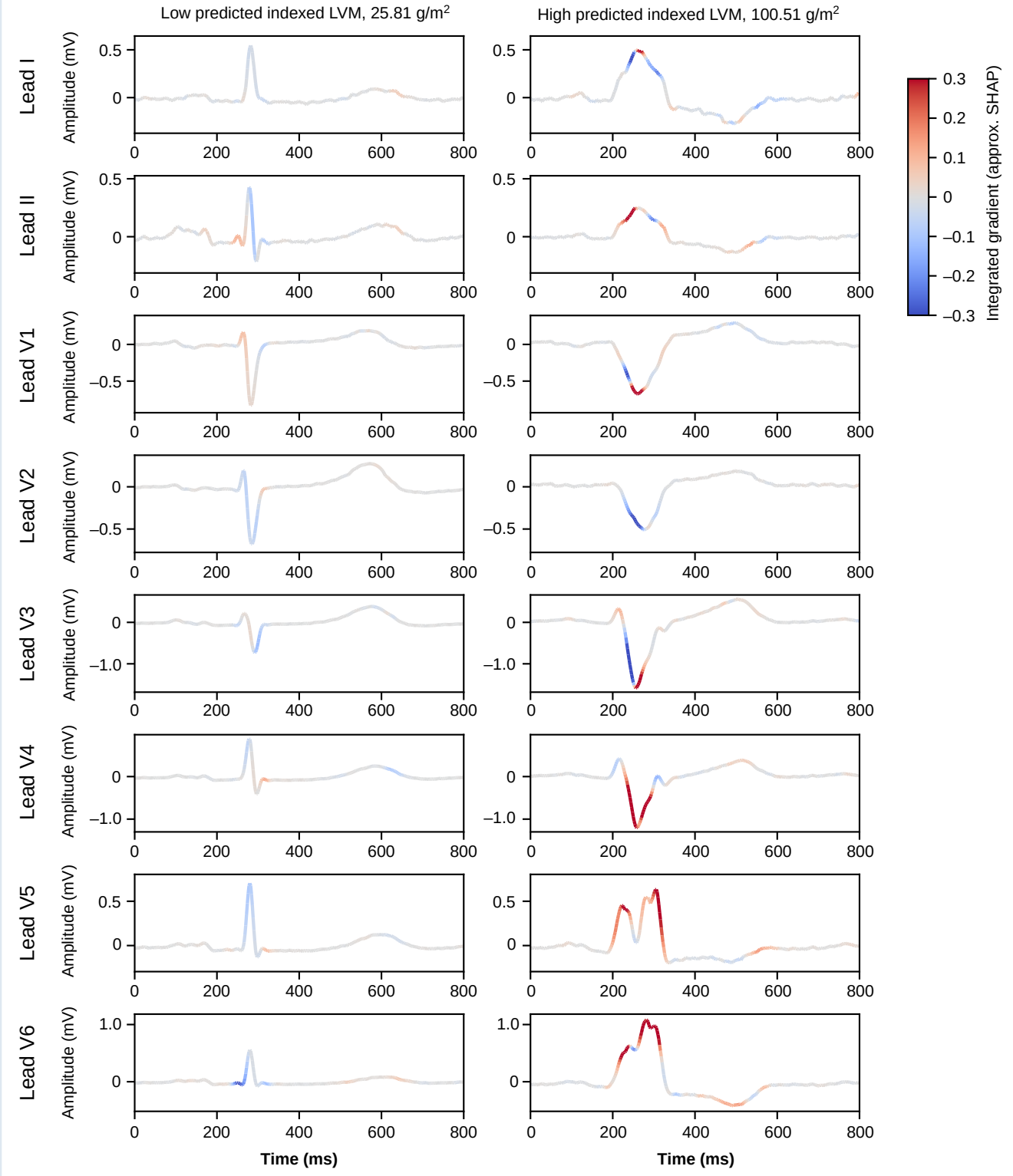


**Figure 5** Approximated SHAP values (integrated gradients) for two participants' median ECGs from the UKB test set, with low (left) and high (right) predicted indexed LVM respectively. Colours correspond to morphology effect, red increasing predictions and blue decreasing predictions, and grey having little relative effect. ECG, electrocardiogram; LVM, left ventricular mass; SHAP, SHapley Additive exPlanations; UKB, UK Biobank.

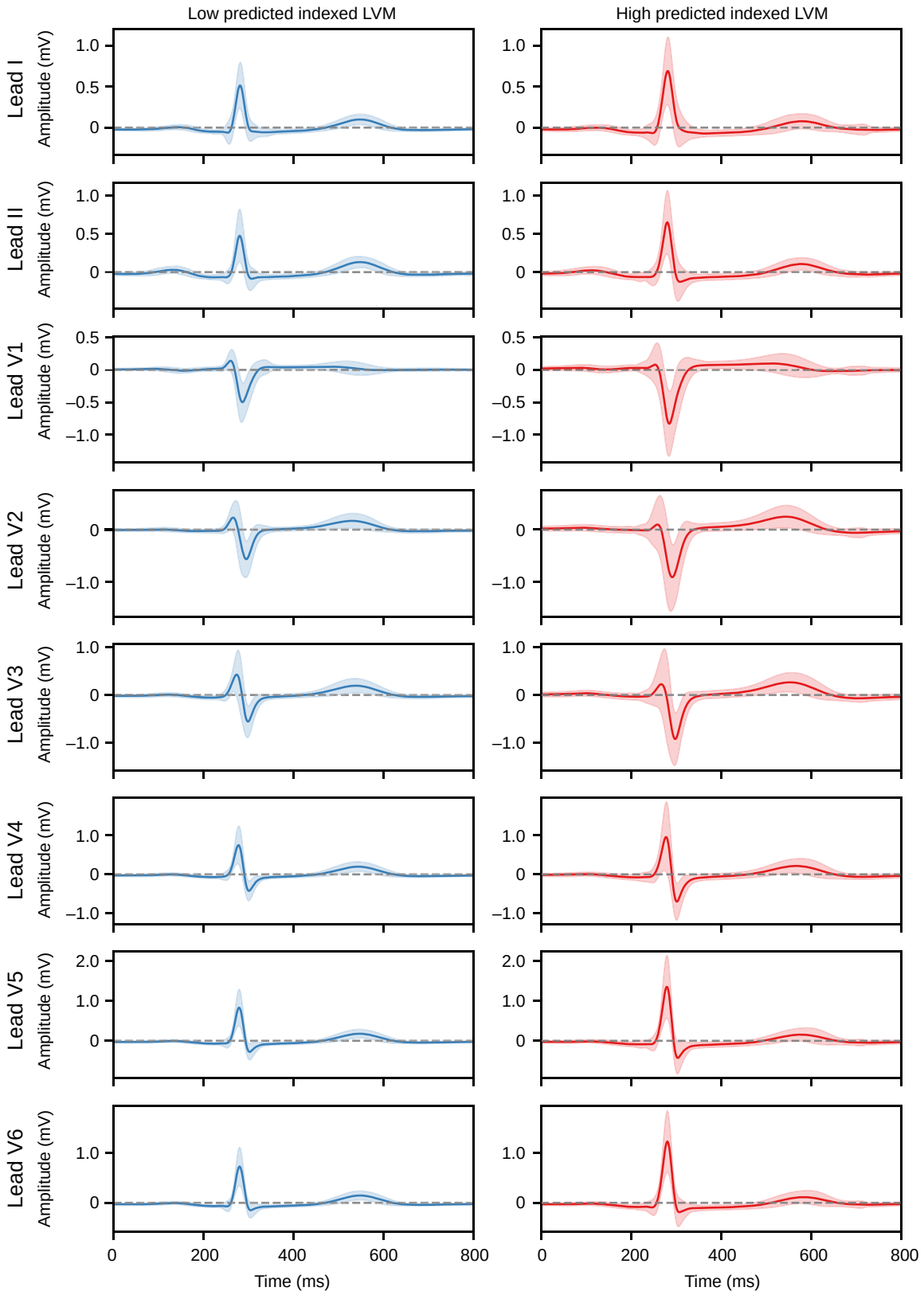


**Figure 6** Mean ECG waveforms across participants from the UKB test set with low (below 5th percentile) or high (above 95th) percentile predicted indexed LVM. The shaded region corresponds to lower and upper SD bounds. ECG, electrocardiogram; LVM, left ventricular mass; SD, standard deviation; UKB, UK Biobank.

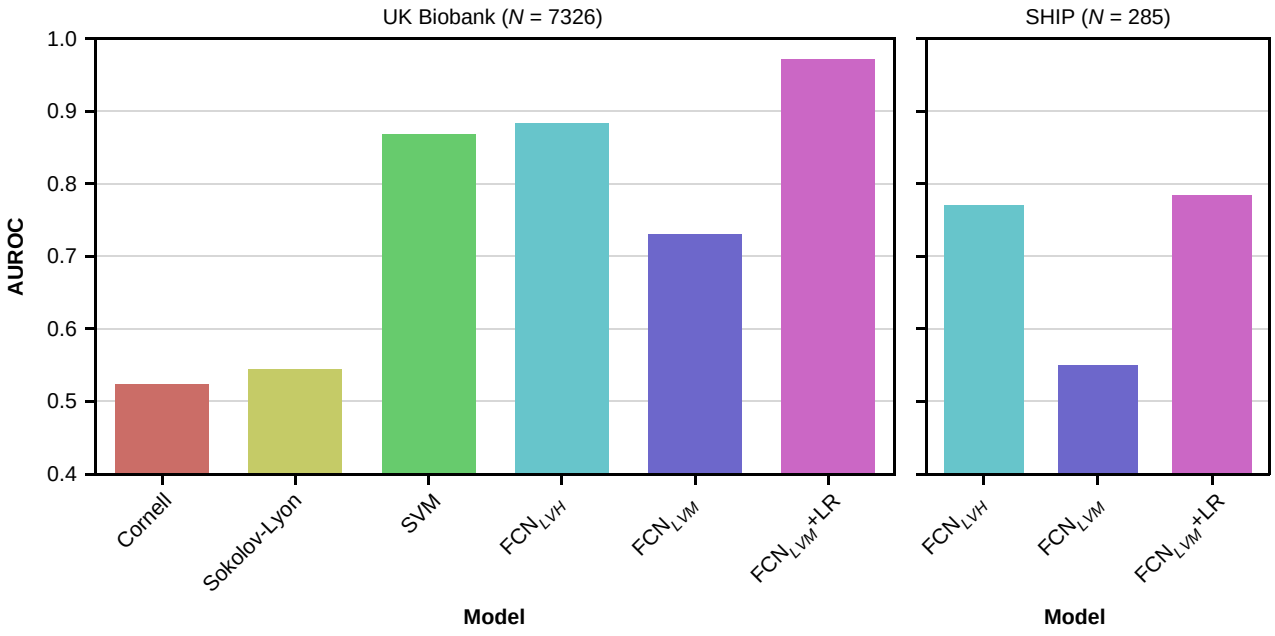


**Figure 7** AUROC comparison in UKB and SHIP test sets. AUROC, area under the receiver operator curve, SHIP, Study of Health in Pomerania; UKB, UK Biobank.

disease phenotypes associated with LVH, rather than a direct mechanistic driver. Furthermore, the ECG-only configuration of DL models demonstrated robust performance, reinforcing the value of the raw ECG waveform for LVH prediction.

## Comparison to contemporary studies

There have been other contemporary studies that have also applied DL to ECG data for LVH prediction,[43,44] and two using UKB.[10,11] Khurshid et al. (2021) developed a 10-layer convolutional neural network (CNN) with residual connections to predict CMR-derived LVM from the ECG (entire 10 s) in 37 142 UKB participants with a c-statistic of 0.65 [0.61–0.70] (sensitivity = 0.34 [0.25, 0.44], specificity = 0.96 [0.96–0.97]), a similar predictive profile to that of the $FCN_{LVM}$ in our present work.[10] External validation was sought in 1371 patients from Mass General Brigham with a c-statistic of 0.62 [0.59–0.65] (sensitivity = 0.41 [0.36–0.46], specificity = 0.83 [0.80–0.86]), following a linear recalibration of LVM predictions with sex as a covariate. Radhakrishnan et al. (2023) developed a multi-modal model with separate CNNs for ECGs (1.2 s median beat) and MRIs, but a unified (cross-modal) latent space, allowing unimodal inference of several clinical phenotypes from the ECG alone in 38 686 UKB participants. In the case of LVH, they achieved an AUROC of 0.72 [0.70–0.73]. Our study outperformed these previous efforts whilst maintaining high sensitivity and specificity. Incorporating an LR step that recalibrated predictions using sex as a covariate significantly improved classification performance by adjusting decision thresholds, resembling the linear LVM recalibration step used by Khurshid et al. in external validation. This hybrid approach, which blends regression and classification methods, offered a flexible and interpretable mechanism for refining predictions in skewed populations. Notably, the use of an LR model, as opposed to a linear recalibration of iLVM predictions, offers the flexibility of an adaptive iLVM cut-off for LVH classification, accounting for distributional differences in iLVM predictions vs. CMR-derived iLVM. It is possible that reducing the dimensionality of the ECG waveform into a median beat, as opposed to analysing the entire 10-s waveform, simplified LVM prediction and enabled our use of a relatively small CNN (in terms of convolutional blocks) compared with previous studies. Analysing just a median beat might have also simplified training using the UKB sample, given the sample size is limited despite having increased in size since the previous studies, i.e. using the entire ECG might have necessitated a larger sample or pre-training. The modest generalizability of our model likely reflects domain shifts between cohorts, including demographic differences, ECG acquisition protocols, and downstream imaging analysis. Notably, the papillary muscles were excluded in the UKB CMR image analysis, in contrast to SHIP.[13,45] These differing image analysis protocols may in part explain the prevalence of LVH in the cohorts and the DL model generalizability. Despite methodological considerations to address overfitting, it is possible that a degree of overfitting to the UKB sample (as the sole training dataset) also hindered generalization in SHIP. One promising approach to improve generalizability in future work will be to leverage foundation models with large-scale pre-training across millions of ECGs (not necessarily with paired CMR), which should rapidly adapt to specific tasks such as LVH detection in new datasets.[46–48]

Outside of the UKB, similar performance for LVH detection from ECGs has been reported in a few studies, but all in clinical cohorts and without external validation, making it challenging to directly compare approaches. Liu et al. (2023) studied ECGs from the Tri-service General Hospital Songshan Branch (Taipei, Taiwan), but their approach differed by using 24 derived ECG features as input to a small fully connected neural network (sensitivity = 0.97, specificity = 0.96).[49] Kashou et al. (2020) studied a vast cohort from the Mayo Clinic ECG laboratory (*N* = 720 978), using a residual network with 33 convolutional

layers (AUROC = 0.99, sensitivity = 0.96, and specificity = 0.94)[50]. Hughes et al. (2021) studied ECGs from the University of California, San Francisco, again using a large residual network (AUROC = 0.98, sensitivity = 0.97, and specificity = 0.85)[51]. These studies all report strong diagnostic performance comparable to that of our present study, but we have demonstrated that this does not guarantee generalization in an external cohort. Differences in training cohorts between our study and others might also lead to differing performance profiles dependent on external cohort characteristics, warranting validation in several cohorts. For example, training on a relatively healthy population cohort (UKB) might improve negative predictive value and diagnostic performance for borderline cases, whereas studies trained on higher-risk clinical cohorts might achieve greater sensitivity and accurately predict iLVM in ranges associated with LVH. This suggests that clinical translation of DL models for LVH screening requires training and calibration across both population and higher-risk clinical cohorts.

### Clinical utility

From a clinical perspective, the ECG is a widely accessible, low-cost diagnostic tool used routinely in practice. However, traditional ECG criteria for detecting LVH have limited sensitivity, making them sub-optimal for population-level screening. An artificial intelligence (AI)-enabled ECG model could support LVH detection as a scalable 'front-line' triage tool in settings where cardiac imaging capacity is constrained. For example, in primary care or hypertension clinics, a high-risk AI-ECG LVH score could prompt targeted confirmatory imaging (echocardiography or CMR), review of BP control and secondary causes, and closer follow-up. Conversely, a low-risk score could help deprioritize imaging in low-pre-test probability cases, reducing unnecessary investigations. In cardiology services, the model could be applied opportunistically to existing digital ECG archives to identify previously unrecognized patients who may benefit from risk factor optimization or evaluation for cardiomyopathy phenotypes. These potential workflows align with broader trends in digital cardiology where interoperable infrastructures, remote care pathways and scalable analytics are increasingly leveraged to triage large volume of longitudinal data and support more efficient, earlier risk identification, as highlighted in the recent EHRA summit.[52] Future work should focus on prospective validation in diverse clinical settings, integration into electronic health records systems to enable automated flagging of high-risk individuals in routine care. It should also explore dynamic, risk-based thresholds that incorporate serial CGS and evolving clinical parameters. There is scope to integrate other features such as proteomics, metabolomics, biochemistry, and genetic risk scores to further personalize the model.

### Limitations

Our study has limitations that warrant discussion. Firstly, participants in UKB and SHIP are predominantly of white European ancestry and have limited data (especially SHIP); therefore, further training and validation across large and diverse ethnic populations with differing risk profiles would improve the fairness (inclusion) of future studies and might improve generalization and optimize performance across populations. This issue of participant homogeneity is evidenced by our fine-tuning of models trained in UKB as part of external evaluation in SHIP. Second, although we used a common method to adjust BP measurements for treatment effects from antihypertensive therapy,[18] we acknowledge the limitation of uniform correction factors and the potential variability due to individual responses.

## Conclusions

The DL model integrating ECG and clinical variables effectively classified CMR-derived LVH, outperforming both previously developed supervised algorithms and current clinical ECG benchmarks. The model demonstrated moderate generalizability to an external community-based population, although differences in clinical characteristics and ECG acquisition methods impaired performance, emphasizing the need for model training across larger datasets with greater diversity ahead of further validation and broader deployment. Our findings support the feasibility of developing scalable, DL-based ECG screening tools for the prediction of LVH, whilst highlighting key considerations ahead of translation into a clinical setting.

### Ethics statement

This study complies with the Declaration of Helsinki; the work was covered by the ethical approval for UK Biobank studies from the NHS National Research Ethics Service on 17th June 2011 (Approval number 11/NW/0382) and extended on 18 June 2021 (Approval number 21/NW/0157) with written informed consent obtained from all participants. The work related to the Study of Health in Pomerania is via application reference number SHIP/2023/31/D. The study is covered by the overall ethical approval for SHIP studies approved by the Ethics Committee at the University Medicine Greifswald, Germany.

## Supplementary material

Supplementary material is available at *Europace* online.

## Author contributions

H.N, T.K., and P.B.M. conceptualized the study; H.N., T.K., P.B.M., and J.R. developed the methodology; H.N. and T.K. collected the data; H.N. and T.K. wrote the original draft; all co-authors critically reviewed the manuscript. H.N. and T.K. are co-first authors.

### Acknowledgements

This study was conducted using the UK Biobank resource under access application 2964. This work uses data provided by patients and collected by the NHS as part of their care and support. We would like to thank all the participants, staff involved with planning, collection and analysis, including core lab analysis of the CMR imaging data.

### Funding

HN acknowledges the British Heart Foundation Pat Merriman Clinical Research Training Fellowship (FS/20/22/34 640) and the National Institute for Health and Care Research's (NIHR) Integrated Academic Training Programme, which supports his Academic Clinical Lectureship post (CL-2024-19-002). JR acknowledges fellowship RYC2021-031413-I from the European Union 'NextGenerationEU/PRTR' and MCIN/AEI/10.13039/501100011033 and grants PID2023-148975OB-I00 and CNS2023-143599 funded by the Spanish Ministry of Science and Innovation and FEDER. NA acknowledges support from the Medical Research Council for his Clinician Scientist Fellowship (MR/X020924/1). SEP acknowledges the British Heart Foundation for funding the manual analysis to create a cardiovascular magnetic resonance imaging reference standard for the UK Biobank imaging resource in 5000 CMR scans (www.bhf.org.uk, project reference PG/14/89/31194). TK, SEP, and PBM acknowledge support from the National Institute for Health and Care Research (NIHR) Barts

Biomedical Research Centre (NIHR202330); a delivery partnership of Barts Health NHS Trust, Queen Mary University of London, St George's University Hospitals NHS Foundation Trust, and St George's University of London. SEP, KL, and ER have received funding from the European Union's Horizon 2020 research and innovation programme under grant agreement No 825903 (euCanSHare project). KL has received funding from the European Union's Horizon 2020 research and innovation programme under grant agreements No 101080430 (AI4HF project) and No. 101057849 (DataTools4Heart project). SvD is funded by the Oxford British Heart Foundation Centre of Research Excellence. The Study of Health in Pomerania (SHIP) is part of the Community Medicine Research net (CMR) (https://www.unimedizin-greifswald.de/icm/) of the University Medicine Greifswald, which is supported by the German Federal Ministry of Education and Research (BMBF, grant numbers: 01ZZ96030 and 01ZZ0701) and the Federal State of Mecklenburg-West Pomerania. MRI scans in SHIP-2 and SHIP-TREND-0 have been supported by a joint grant from Siemens Healthineers, Erlangen, Germany and the Federal State of Mecklenburg-West Pomerania. This study was carried out in collaboration with the German Centre for Cardiovascular Research (DZHK), which is supported by the German Federal Ministry of Education and Research (BMBF).

**Conflict of interest:** SEP provides consultancy to and owns stock of Cardiovascular Imaging Inc, Calgary, Alberta, Canada. All remaining authors have declared no conflicts of interest.

## Data availability

The data underlying this article were provided by the UK Biobank under access application 2964. UK Biobank will make the data available to bona fide researchers for all types of health-related research that is in the public interest, without preferential or exclusive access for any persons. All researchers will be subject to the same application process and approval criteria as specified by UK Biobank. For more details on the access procedure, see the UK Biobank website: http://www.ukbiobank.ac.uk/register-apply/. Code for running the experiments, analysis and plotting is available on a Zenodo repository: https://github.com/Electrogenomics-Group/ai-ecg-lvh. This open-source resource is intended solely for research purposes and has not been approved for use by any legal authority.

## References

1. Levy D, Garrison RJ, Savage DD, Kannel WB, Castelli WP. Prognostic implications of echocardiographically determined left ventricular mass in the Framingham Heart Study. *N Engl J Med* 1990;**322**:1561–6.
2. Haider AW, Larson MG, Benjamin EJ, Levy D. Increased left ventricular mass and hypertrophy are associated with increased risk for sudden death. *J Am Coll Cardiol* 1998;**32**:1454–9.
3. Pewsner D, Jüni P, Egger M, Battaglia M, Sundström J, Bachmann LM. Accuracy of electrocardiography in diagnosis of left ventricular hypertrophy in arterial hypertension: systematic review. *BMJ* 2007;**335**:711.
4. Okin PM, Roman MJ, Devereux RB, Kligfield P. Electrocardiographic identification of increased left ventricular mass by simple voltage-duration products. *J Am Coll Cardiol* 1995;**25**:417–23.
5. Bacharova L, Estes EH. Left ventricular hypertrophy by the surface ECG. *J Electrocardiol* 2017;**50**:906–8.
6. Naderi H, Ramírez J, van Duijvenboden S, Pujadas ER, Aung N, Wang L *et al.* Predicting left ventricular hypertrophy from the 12-lead electrocardiogram in the UK Biobank imaging study using machine learning. *Eur Heart J Digit Health* 2023;**4**:316–24.
7. Attia ZI, Kapa S, Lopez-Jimenez F, McKie PM, Ladewig DJ, Satam G *et al.* Screening for cardiac contractile dysfunction using an artificial intelligence-enabled electrocardiogram. *Nat Med* 2019;**25**:70–4.
8. Hannun AY, Rajpurkar P, Haghpanahi M, Tison GH, Bourn C, Turakhia MP *et al.* Cardiologist-level arrhythmia detection and classification in ambulatory electrocardiograms using a deep neural network. *Nat Med* 2019;**25**:65–9.
9. Wei-Yin Ko MS, Konstantinos C, Siontis MD, Zachi I, Attia M, Rickey E *et al.* Detection of hypertrophic cardiomyopathy using a convolutional neural network-enabled electrocardiogram. *J Am Coll Cardiol* 2020;**75**:722–33.
10. Khurshid S, Friedman S, Pirruccello JP, Di Achille P, Diamant N, Anderson CD *et al.* Deep learning to predict cardiac magnetic resonance–derived left ventricular mass and hypertrophy from 12-lead ECGs. *Circ Cardiovasc Imaging* 2021;**14**:e012281.
11. Radhakrishnan A, Friedman SF, Khurshid S, Ng K, Batra P, Lubitz SA *et al.* Cross-modal autoencoder framework learns holistic representations of cardiovascular state. *Nat Commun* 2023;**14**:2436.
12. Svennberg E, Han JK, Caiani EG, Engelhardt S, Ernst S, Friedman P *et al.* State of the art of artificial intelligence in clinical electrophysiology in 2025: a scientific statement of the European Heart Rhythm Association (EHRA) of the ESC, the Heart Rhythm Society (HRS), and the ESC Working Group on E-Cardiology. *Europace* 2025;**27**:euaf071.
13. Petersen SE, Aung N, Sanghvi MM, Zemrak F, Fung K, Paiva JM *et al.* Reference ranges for cardiac structure and function using cardiovascular magnetic resonance (CMR) in Caucasians from the UK Biobank population cohort. *J Cardiovasc Magn Reson* 2017;**19**:18.
14. Bai W, Sinclair M, Tarroni G, Oktay O, Rajchl M, Vaillant G *et al.* Automated cardiovascular magnetic resonance image analysis with fully convolutional networks. *J Cardiovasc Magn Reson* 2018;**20**:65.
15. Mosteller RD. Simplified calculation of body-surface area. *N Engl J Med* 1987;**317**:1098.
16. Antonio de Marvao MBC, Kathryn A, McGurk P, Sean L, Zheng BMBC, Marjola Thanaj P *et al.* Phenotypic expression and outcomes in individuals with rare genetic variants of hypertrophic cardiomyopathy. *J Am Coll Cardiol* 2021;**78**:1097–110.
17. Lopes LR, Aung N, van Duijvenboden S, Munroe PB, Elliott PM, Petersen SE. Prevalence of hypertrophic cardiomyopathy in the UK Biobank population. *JAMA Cardiol* 2021;**6**:852–4.
18. Tobin MD, Sheehan NA, Scurrah KJ, Burton PR. Adjusting for treatment effects in studies of quantitative traits: antihypertensive therapy and systolic blood pressure. *Stat Med* 2005;**24**:2911–35.
19. Nissen SE, Tuzcu EM, Schoenhagen P, Crowe T, Sasiela WJ, Tsai J *et al.* Statin therapy, LDL cholesterol, C-reactive protein, and coronary artery disease. *N Engl J Med* 2005;**352**:29–38.
20. Wang Z, Yan W, Oates T. Time series classification from scratch with deep neural networks: A strong baseline. *Int J Conf Neural Netw (IJCNN)* 2017:1578–85. doi: 10.1109/IJCNN.2017.7966039
21. Ismail Fawaz H, Forestier G, Weber J, Idoumghar L, Muller P-A. Deep learning for time series classification: a review. *Data Min Knowl Disc* 2019;**33**:917–63.
22. Soto JT, Weston Hughes J, Sanchez PA, Perez M, Ouyang D, Ashley EA. Multimodal deep learning enhances diagnostic precision in left ventricular hypertrophy. *Eur Heart J Digit Health* 2022;**3**:380–9.
23. Avula V, Wu KC, Carrick RT. Clinical applications, methodology, and scientific reporting of electrocardiogram deep-learning models: a systematic review. *JACC Adv* 2023;**2**:100686.
24. Python Software Foundation. Python Language Reference, Version 3.11.11, 2025. http://www.python.org (18 June 2025, date last accessed).
25. Paszke A, Gross S, Massa F, Lerer A, Bradbury J, Chanan G, *et al.* PyTorch: an imperative style, high-performance deep learning library. In Proceedings of the 33rd International Conference on Neural Information Processing Systems Dec 8 2019:8026–37.
26. Liaw R, Liang E, Nishihara R, Moritz P, Gonzalez JE, Stoica I. Tune: a research platform for distributed model selection and training. arXiv.org. 2018. https://arxiv.org/abs/1807.05118v1 (14 May 2025).
27. Zhou Y, Cosentino J, Yun T, Biradar MI, Shreibati J, Lai D, *et al.* Applying multimodal AI to physiological waveforms improves genetic prediction of cardiovascular traits. . *Am J Hum Genet* 2025;**112**:1562–79. doi:10.1016/j.ajhg.2025.05.015
28. Sokolow M, Lyon TP. The ventricular complex in left ventricular hypertrophy as obtained by unipolar precordial and limb leads. *Am Heart J* 1949;**37**:161–86.
29. Casale PN, Devereux RB, Kligfield P, Eisenberg RR, Miller DH, Chaudhary BS *et al.* Electrocardiographic detection of left ventricular hypertrophy: development and prospective validation of improved criteria. *J Am Coll Cardiol* 1985;**6**:572–80.
30. Völzke H. Study of Health in Pomerania (SHIP). *Bundesgesundheitsbl* 2012;**55**:790–4.
31. Holger KS, Kern S, Orfanos DP, Vallat R, Brunner C, Cerina L, *et al.* holgern/pyedflib: v0.1.40. *Zenodo* 2025. doi.org/10.5281/zenodo.14957195
32. Lekadir K, Frangi AF, Porras AR, Glocker B, Cintas C, Langlotz CP *et al.* FUTURE-AI: international consensus guideline for trustworthy and deployable artificial intelligence in healthcare. *BMJ* 2025;**388**:e081554.
33. Gildenblat J. A python library for confidence intervals. GitHub. https://github.com/jacobgil/confidenceinterval (18 June 2025, date last accessed).
34. Takahashi K, Yamamoto K, Kuchiba A, Koyama T. Confidence interval for micro-averaged F 1 and macro-averaged F 1 scores. *Appl Intell (Dordr)* 2022;**52**:4961–72.

35. Zou L, Choi Y-H, Guizzetti L, Shu D, Zou J, Zou G. Extending the DeLong algorithm for comparing areas under correlated receiver operating characteristic curves with missing data. *Stat Med* 2024;**43**:4148–62.
36. Sundararajan M, Taly A, Yan Q. Axiomatic attribution for deep networks (ed.), *Proc Mach Learn Res*. Proceedings of the 34th International Conference on Machine Learning (ICML). Sydney, Australia; 2017. p. 3319–28 70.
37. Lundberg SM, Lee S-I. A unified approach to interpreting model predictions. *In: Proceedings of the 31st International Conference on Neural Information Processing Systems (NeurIPS/NIPS 2017)* 2017:4768–77.
38. Yuan H, Liu M, Kang L, Miao C, Wu Y. An empirical study of the effect of background data size on the stability of SHapley Additive exPlanations (SHAP) for deep learning models. arXiv; 2023.
39. Molloy TJ, Okin PM, Devereux RB, Kligfield P. Electrocardiographic detection of left ventricular hypertrophy by the simple QRS voltage-duration product. *J Am Coll Cardiol* 1992;**20**:1180–6.
40. Bacharova L, Szathmary V, Kovalcik M, Mateasik A. Effect of changes in left ventricular anatomy and conduction velocity on the QRS voltage and morphology in left ventricular hypertrophy: a model study. *J Electrocardiol* 2010;**43**:200–8.
41. Gonzales TI, Jeon JY, Lindsay T, Westgate K, Perez-Pozuelo I, Hollidge S *et al.* Resting heart rate is a population-level biomarker of cardiorespiratory fitness: the Fenland Study. *PLoS One* 2023;**18**:e0285272.
42. Ma Y, Qi M, Li K, Wang Y, Ren F, Gao D. Conventional and genetic associations between resting heart rate, cardiac morphology and function as assessed by magnetic resonance imaging: insights from the UK Biobank population study. *Front Cardiovasc Med* 2023;**10**:1110231
43. Rabkin SW. Searching for the best machine learning algorithm for the detection of left ventricular hypertrophy from the ECG: a review. *Bioengineering (Basel)* 2024;**11**:489.
44. Siranart N, Deepan N, Techasatian W, Phutinart S, Sowalertrat W, Kaewkanha P *et al.* Diagnostic accuracy of artificial intelligence in detecting left ventricular hypertrophy by electrocardiograph: a systematic review and meta-analysis. *Sci Rep* 2024;**14**:15882.
45. Bülow R, Ittermann T, Dörr M, Poesch A, Langner S, Völzke H *et al.* Reference ranges of left ventricular structure and function assessed by contrast-enhanced cardiac MR and changes related to ageing and hypertension in a population-based study. *Eur Radiol* 2018;**28**:3996–4005.
46. Han Y, Liu X, Zhang X, Ding C. Foundation models in electrocardiogram: a review. arXiv; 2024.
47. Li J, Aguirre A, Moura J, Liu C, Zhong L, Sun C, *et al.* An electrocardiogram foundation model built on over 10 million recordings. *N Eng J Medi AI* 2025; **2**. doi: 10.1056/aioa2401033
48. Wan Z, Yu Q, Mao J, Duan W, Ding C. OpenECG: benchmarking ECG foundation models with public 1.2 million records. arXiv.org. 2025. https://arxiv.org/abs/2503.00711v1 (18 June 2025).
49. Liu C-W, Wu F-H, Hu Y-L, Pan R-H, Lin C-H, Chen Y-F *et al.* Left ventricular hypertrophy detection using electrocardiographic signal. *Sci Rep* 2023;**13**: 1–13.
50. Kashou AH, Medina-Inojosa JR, Noseworthy PA, Rodeheffer RJ, Lopez-Jimenez F, Attia IZ, *et al.* Artificial intelligence-augmented electrocardiogram detection of left ventricular systolic dysfunction in the general population. *Mayo Clin Proc* 2021;**96**:2576–86. doi: 10.1016/j.mayocp.2021.02.029
51. Hughes JW, Olgin JE, Avram R, Sittler T, Radia K, *et al.* Performance of a convolutional neural network and explainability technique for 12-lead electrocardiogram interpretation. *JAMA Cardiol* 2021;**6**:1285–95. doi: 10.1001/jamacardio.2021.2746
52. Traykov V, Puererfellner H, Burri H, Foldesi CL, Scherr D, Duncker D *et al.* EHRA perspective on the digital data revolution in arrhythmia management: insights from the association's annual summit. *Europace* 2025;**27**:euaf149.